University of Delaware
Newark, De 19716-3820
Ph: 302/831-6200
Fax: 302/831-6226
www.udel.edu/iec

INSTITUTE OF ENERGY CONVERSION

UNITED STATES DEPARTMENT OF ENERGY
UNIVERSITY CENTER OF EXCELLENCE
FOR PHOTOVOLTAIC RESEARCH AND EDUCATION

July 31, 2006

Ken Zweibel
National Renewable Energy Laboratory
1617 Cole Boulevard
Golden, CO 80401

Re: NREL Subcontract #ADJ-1-30630-12
D.5.3

Dear Ken,

This report covers research conducted at the Institute of Energy Conversion (IEC) for the period from April 16, 2006 to May 15, 2006, under the subject subcontract. The report highlights progress and results obtained under Task 1 (CdTe-based solar cells).

Task 1 – CdTe-based Solar Cells

Summary

The CdTe task is establishing a baseline fabrication process for high efficiency cells with high processing throughput on commercial glass/TCO. During this reporting period, CdTe cell fabrication focused on evaluation of alternative high resistance (HR) buffer layers and the influence of ambient composition during vapor transport (VT) CdTe deposition and vapor $CdCl_2$ treatment. Aspects of CdTe surface chemistry were investigated with respect to rapid vapor $CdCl_2$ treatment and aniline etching. Bifacial solar cell analysis of cells with different CdTe thickness was carried out to provide detailed understanding of device operation and its relation to processing optimization.

Influence of Buffer Layer Composition on VT CdTe/CdS Solar Cells

High resistance (HR) buffer layers such as intrinsic SnO_2, Ga_2O_3 and Al_2O_3 between the doped SnO_2:F and CdS have been widely applied in CdTe cells. Without the HR buffer, V_{oc} decreases as CdS thickness decreases. In the past 2 years, we have been using a process for Ga_2O_3 developed at IEC where Ga is sputtered (SP) onto Tec15 SnO_2:F substrates, then reacted in O_2 to form the sesquioxide Ga_2O_3. However, problems with the SP-Ga_2O_3 HR layer have been identified and correlated with poor device performance and shunting. This forced a re-evaluation of HR buffer formation and processing.

Compositional analysis found Cu contamination in the sputtered Ga films, believed to be related to sputtering from liquid Ga held in a Cu cup. Alternative HR layer processes were sought, both with alternative Ga deposition and use of other materials, in particular Al_2O_3. We have developed a method to form Ga_2O_3 using electrodeposition (ED) followed by reaction in O_2 at 550°C. Al_2O_3 HR layers were fabricated using electron-beam evaporated Al followed by reaction in O_2 at 550°C. We focus here on results from the Ga_2O_3 layers. Materials properties of the ED-Ga_2O_3 were very promising. CdS growth on the ED Ga_2O_3 was very uniform and dense. After CdTe growth, no pin-holes were found over the 10 cm x 10 cm deposition.

Figure 1 shows the light and dark JV curves for cells from two recent VT runs. VT201 incorporated the previous HR method, SP-Ga_2O_3 while VT237 incorporated a new ED-Ga_2O_3. Both runs had similar CdS and CdTe conditions and were co-processed through $CdCl_2$ treatment and contacting so that the only difference was the HR layer. VT201 has significant light-to-dark crossover, which we have shown can be due to photoconductive CdS (PC-CdS). Cu-doping is perhaps the most common method to create PC-CdS. We have previously shown that a signature of PC-CdS is the significant increase in apparent QE between 400 and 520 nm with forward bias and light bias, often leading to QE>1[i]. Figure 2 shows the apparent QE for the same device from VT201 measured with 0V and 0.5V with red light bias. The signature of PC-CdS is consistent with Cu-contaminated CdS where the Cu came from the Ga. The other device with ED-Ga_2O_3 had a negligible PC-CdS effect.

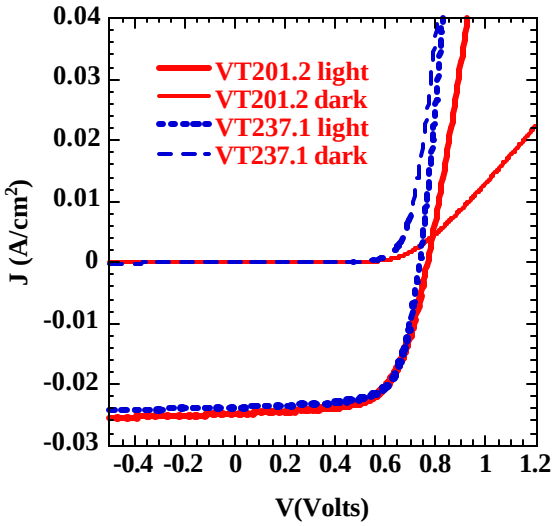

Figure 1. Light and dark JV curves for devices from VT201 (SP-Ga_2O_3) and VT237 (ED-Ga_2O_3).

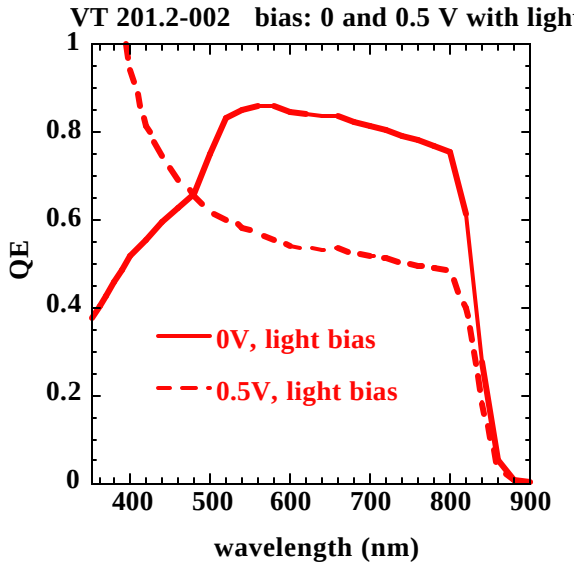

Figure 2. Apparent QE for device from VT201 showing typical signature of PC-CdS with red bias light at forward bias.

Devices in run VT238 had double the ED-Ga_2O_3 thickness (60 nm) from that in VT237 (30 nm). Table I shows the JV performance for these three devices and several others discussed below. Figure 3 shows the QE at 0V dark bias for VT237 and VT238. They are identical, indicating no additional optical absorption due to the Ga_2O_3. The table indicates they have similar JV performance, notably high FF. Figure 3 also shows the QE for two CdTe devices deposited on borosilicate glass/SnO_2 with intrinsic SnO_2 HR buffer layers produced at NREL by Dr X. Li. VT226 was processed with the standard CSD CdS thickness (90 nm) while VT227 had only 60 nm CdS. As expected, the V_{oc} and yield were lower for the sample with thinner CdS; without the buffer layer, these CdS thicknesses would yield cells with V_{oc} < 500 mV. However, J_{sc} was higher due to higher blue response with the thinner CdS as seen in Figure 3. Table I also includes results on a piece having a 60 nm thick Al_2O_3 HR layer, VT217, showing similar performance to those with Ga_2O_3.

From the QE in Figure 3, it is apparent that the NREL glass/SnO_2 is optically superior to the Tec 15 in both the blue and the red regions. We have quantified this effect by comparing the integrated QE in different regions from VT226 (NREL) and VT238 (Tec 15), which both had 3 layers of CdS. Between 350 and 540 nm, VT226 had about 1 mA/cm^2 higher current due to the increased blue response. Between 560 and 900 nm, VT226 also had about 1 mA/cm^2 higher current due to the increased red response. This accounts for the approximately 2 mA/cm^2 higher J_{sc} under AM1.5 simulated sunlight for the devices on NREL borosilicate glass with their SnO_2. Decreasing the CdS to only 2 coats as in VT227 results in a gain of another 0.7 mA/cm^2 between 350 and 540 nm compared to VT226 but with a loss in V_{oc}, FF and yield.

Table I. JV performance for recent VT CdS/CdTe devices having different glass, SnO_2, HR layers, and CdS thickness. QE for these devices are in Figure 3. NREL=borosilicate glass with SnO_2:F and intrinsic SnO_2 HR deposited at NREL. VT226, VT227 and VT238 were co-processed while VT201 and 237 were co-processed. Yield was defined by the number of cells with low shunt conductance, i.e. G_{sc}< 5 mS/cm^2.

Piece	Glass/ SnO_2	HR	CdS layers	V_{oc}	J_{sc}	FF	Eff.	Yield
VT226.1	NREL	i-SnO_2	3X	0.772	25.6	68.6	13.6	4/6
VT227.1	NREL	i-SnO_2	2X	0.632	26.8	61.3	10.4	1/6
VT201.2	Tec 15	SP-Ga_2O_3	3X	0.769	24.9	64.6	12.4	6/8
VT217.	Tec 15	EB-Al_2O_3	3X	0.760	24.6	62.6	11.7	7/8
VT237.1	Tec 15	ED-Ga_2O_3	3X	0.737	23.8	70.0	12.3	7/8
VT238.1	Tec 15	ED-Ga_2O_3	3X	0.776	23.9	68.7	12.8	8/8

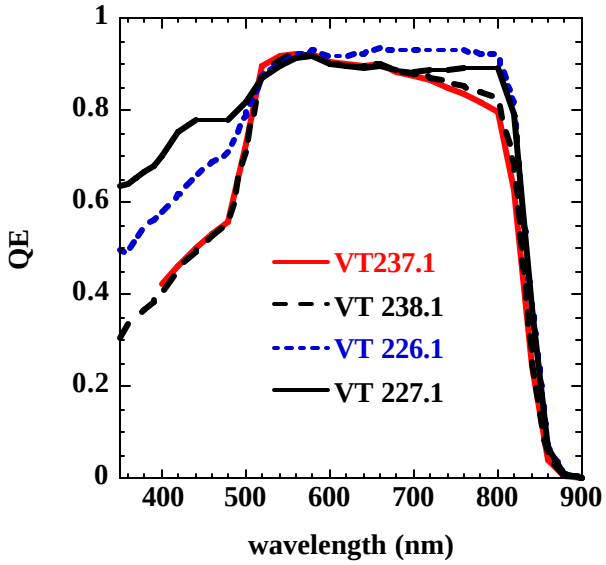

Figure 3. QE at 0V, dark for devices listed in Table I. VT226 and VT227 are on borosilicate glass with SnO_2 from NREL while VT237 and 238 are on Tec15 with Ga_2O_3 HR layers.

Influence of Ambient Composition during CdTe Deposition and $CdCl_2$ Treatment

The previous report (April 2006) showed a dependence of cell performance and uniformity on choice of carrier gases during CdTe VT deposition, with improved uniformity for films deposited in N_2 or Ar ambient compared to He. The carrier gas affects the as-deposited properties of the CdTe and junction. For cells with CdTe deposited by VT and contacted with Cu/Ni directly after deposition (no $CdCl_2$ HT), higher performance is obtained using N_2 or Ar carrier gas for CdTe growth. In Table II

and Figure 4, sample "a" was deposited with He carrier gas and exhibited the usually observed poor J-V behavior and low QE, with a peak in the red. Films deposited in Ar or N_2, on the other hand (sample b) exhibit 10X higher J_{sc} with wide-band collection peaking in the red. To isolate the principal mechanism of these differences, depositions will be carried out at different growth rates and substrate temperatures.

For devices deposited in N_2 ambient, the sensitivity to ambient during the $CdCl_2$ HT was evaluated by varying the partial pressures of $CdCl_2$ vapor and O_2 (in Ar background at total pressure = 1 atm) compared to the baseline. In Table II and Figure 4, sample "e" received the baseline $CdCl_2$ HT with $pCdCl_2$ = 3 mTorr and pO_2 = 150 mTorr, yielding cells with V_{oc} = 800 mV and J_{sc} > 24 mA/cm^2. Reducing the partial pressure of either gas species resulted in lower V_{oc} and J_{sc}, which can be seen in Figure 4 as a nearly panchromatic drop in QE.

Another experiment shed light on the dynamics of the reaction between film and ambient. A cell treated by admitting O_2 to the $CdCl_2$ vapor reactor during the first 20 seconds of a 2 minute HT at 480°C, followed by exposure to only Ar and $CdCl_2$ exhibited high performance, similar to cell "e". A cell treated by admitting O_2 to the reactor for the last 30 seconds of a 2 minute treatment exhibited low photocurrent, hysteresis and blocking contact. It is surmised from this that the short vapor HT works by reaction at the CdTe surface with $CdCl_2$ and O_2 to form defects at the surface, followed by diffusion of these into the film and that the entire optimization protocol for CdTe/CdS is controlling diffusion.

Table II. Solar cell performance for different carrier gas during VT growth and ambient composition during $CdCl_2$ treatment.

Cell	Carrier Gas	$PCdCl_2$ (mTorr)	pO_2 (Torr)	V_{oc} (mV)	J_{sc} (mA/cm^2)
a	He	None	None	550	1.7
b	N_2	None	None	650	9.6
c	N_2	3	$<10^{-6}$	650	23.0
d	N_2	0.1	150	794	23.8
e	N_2	3	150	800	24.8

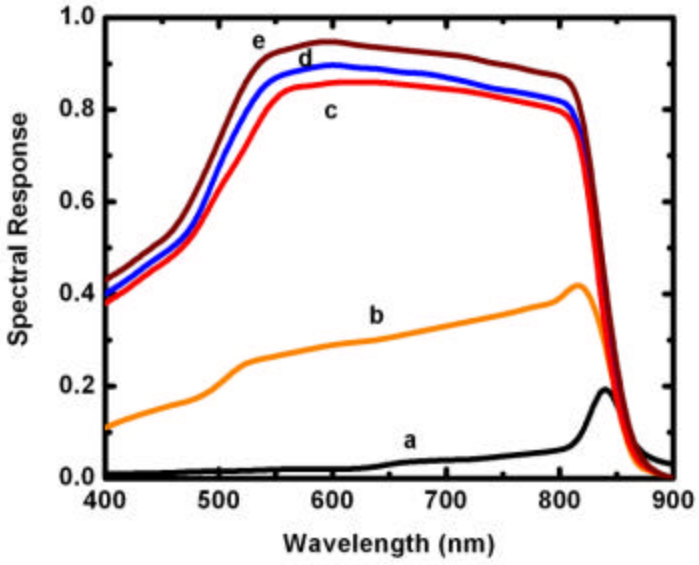

Figure 4. QE (light bias at 0 V) of devices of Table III.

Surface Chemistry in High Throughput Processed CdTe Cells

In the previous report, we showed that CdTe cells with efficiency = 11% having reasonably high FF = 64% could be fabricated with no surface etching or rinsing, provided the $CdCl_2$ vapor treatment was short, ~2 minutes. This surprising result indicates that the relative reaction rates for surface oxidation and carrier production are sufficiently different and that unwanted, excessive, oxidation can be mitigated by using short treatment times at higher temperature. In this case, the CdTe surface is sufficiently conductive to allow contact formation by application of a Cu/metal contact. This offers a substantial pathway forward for processing devices with thin CdTe absorber layers.

The state of and changes in the CdTe surface for films in as-deposited condition, after rapid $CdCl_2$ vapor HT and after etching in aqueous aniline solution were analyzed by contact wetting, x-ray photoemission spectroscopy (XPS) and glancing incidence x-ray diffraction (GIXRD). XPS was measured with a PHI 5300 system using Al kα radiation (1.486 keV) at 15kV and 14 mA and a takeoff angle of 54 deg. Depth profiles were obtained by milling the sample area (1 x 1 cm) with Ar^+ at 2kV and 20 x 10^{-3} Pa, which yields a sputter rate of 13.7 A/min for Ta_2O_5 film standard. GIXRD was measured with a Rigaku D/Max 2000Ultima diffractometer using Cu kα radiation (8.04 keV) at 40 mV and 40 mA at an incident beam angle of 1 deg (sampling depth ~120 nm), scan speed of 0.5 deg/min and step size of 0.02 deg.

The as-deposited film was measured several hours after exposure to room air. The surface was hydrophilic and contained Cd, Te, O, and C, with CdTe and β-$CdTeO_3$ as the only phases. XPS depth profile shows O persisting until ~20 min etch (~30 nm) at which point the the Cd/Te ratio =1 (Figure 5). After $CdCl_2$ vapor HT, the surface remained hydrophilic, the O concentration decreased and additional signal from Cd and Cl were

found on the surface, due to adsorption of Cd-Cl species. XPS depth profile shows no O after ~5 min etch (~7 nm) and a final Cd/Te < 1. GIXRD showed similar phase composition to the as-deposited film. After etching in aniline, the surface became strongly hydrophobic. XPS depth profile showed no O after ~2 min etch (3 nm), a surface Cd/Te = 0.6 and final Cd/Te = 0, indicating the presence of significant Te excess at the surface. GIXRD showed Te and CdTe as the only phases present.

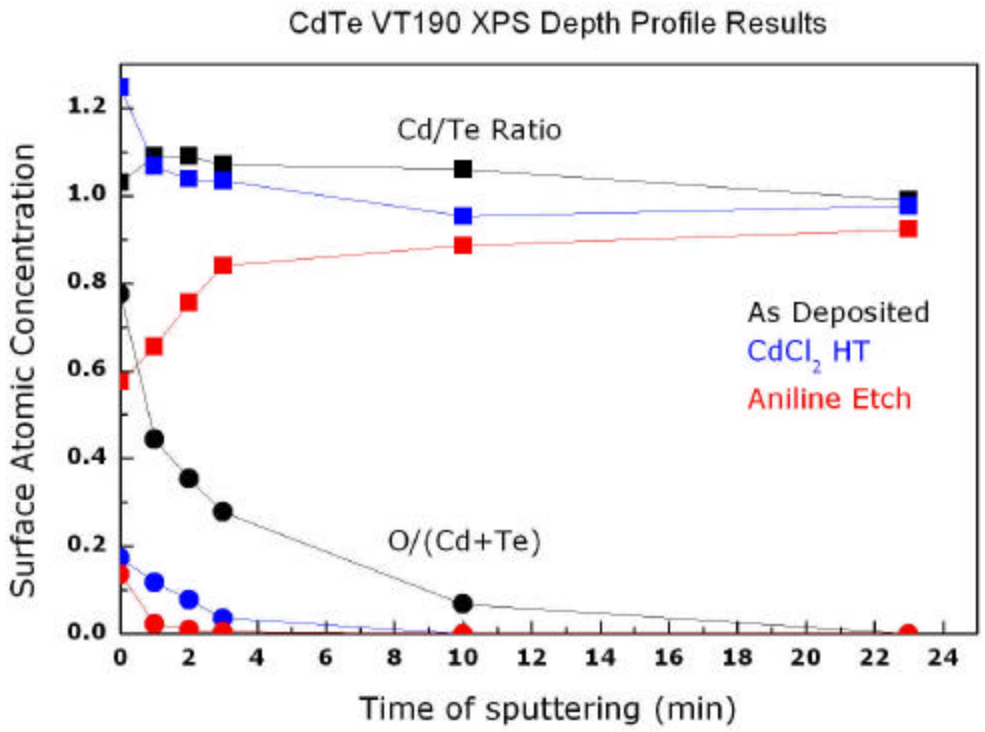

Figure 5. XPS depth profile results for Cd/Te and O/(Cd+Te) for VT deposited CdTe: as-deposited, after 2 minute $CdCl_2$ HT at 480°C, and after 2 minute etch in aniline solution.

The XPS results after the short $CdCl_2$ vapor HT show that the oxide thickness is thin enough for penetration by application of the metal back contact, in contrast to oxides and oxy-chlorides found on CdTe treated with $CdCl_2$ for 20-30 minutes at 380-430°C.

Bifacial CdTe Device Characterization

A summary of the work at IEC on characterization and analysis of bifacial JV and QE using devices with semitransparent ZnTe:Cu back contacts was presented by Darshini Desai at the 4th WCPEC in Hawaii in May 2006. The title of the paper was "How CdTe solar cells operate: determining collection using bifacial device characterization" by D. Desai, S. Hegedus, B. McCandless, R. Birkmire, K. Dobson, D. Ryan. The paper is attached.

Reference:

---

[i] S. Hegedus, D Ryan, K Dobson, D Desai, B McCandless, Mat. Res. Soc. Symp. Proc. **763**, 447 (2003).

Best regards,

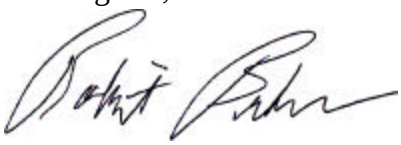

Robert W. Birkmire
Director

RWB/eak

Attachment

Cc: Paula Newton, IEC
Susan Tompkins, OVPR UD
Carolyn Lopez, NREL